

Preparation of (Pb, La)(Zr, Sn, Ti)O₃ antiferroelectric ceramics using colloidal processing and the field induced strain properties

Ming Chen *, Xi Yao, Liangying Zhang

Functional Material Research Laboratory, Tongji University, Shanghai 200092, China

Received 15 September 2000; received in revised form 11 November 2000; accepted 18 November 2000

Abstract

A two-step wet chemical method using colloidal processing was developed for the preparation of (Pb, La)(Zr, Sn, Ti)O₃ antiferroelectric ceramics. The precursor B site was prepared by coprecipitation and precursor A site was introduced in the form of aqueous solution. Dried gel calcined at 600°C for 2 h formed single perovskite phases. Submicron powders were obtained by planetary ball milling. Average grain size about 4 μm and relative density of 98% were achieved from disc specimens sintered at 1100°C for 2 h. An antiferroelectric double polarization hysteresis loop with antiferroelectric to ferroelectric phase revert electric field $E_{AFE-FE} = 4.3$ kV/mm and a strain curve with maximum longitude strain of 0.30% under 6 kV/mm electric field were measured from composition of (Pb_{0.97}La_{0.02})(Zr_{0.65}Sn_{0.25}Ti_{0.10})O₃. © 2001 Elsevier Science Ltd. All rights reserved.

Keywords: Antiferroelectrics; Ferroelectric properties; (Pb, La)(Zr, Sn, Ti)O₃; Perovskites; Powders-chemical preparation

1. Introduction

The lead stannate zirconate titanate (PZST) family of ceramics was first investigated by Berlincourt¹ and has been widely studied for applications in energy conversion in the 60s and 70s.^{2–4} From the beginning of the 80s, the research interest to PZST ceramics was shifted to further understanding the phase transformations and exploring new application potentials of their phase transformation related properties.^{5–13}

In the PZST family, lead lanthanum stannate zirconate titanate (PLZST) and its modifications, which electric field induced structural changes at antiferroelectric to ferroelectric (FE-AFE) phase transformations (e.g. rhombohedral to tetragonal) lead to a maximum 0.85% longitudinal strain,⁶ have been studied for potential actuator applications in recent years.^{10–13}

For the ceramics used in actuators, the purity, stoichiometry, second phase content and grain size which are controlled by the processing conditions, affect markedly the final properties and reliability of the devices.¹⁴ In the

previous studies,^{10–13} the PLZST ceramics were mainly prepared by a conventional solid-state reaction method. Having been proved in PZT ceramics, this kind of method often leads to compositional fluctuation and structural inhomogeneities especially when the composition is near the morphotropic phase boundary.¹⁵

Generally, the wet chemical methods have more advantages in compositional and structural control as compared to the solid-state reaction method. But for the sol-gel method,⁵ the high cost of starting materials and the difficulties in densification caused by a high content of organic materials in the precursors make it more suitable for thin film preparation than for bulk ceramics. As for the PLZST ceramics prepared by coprecipitation,¹³ since lead chloride is quite insoluble, it is difficult to dissolve water soluble lead compound (e.g. lead nitrite and lead acetate) together with the only water soluble stannic compound (e.g. stannic chloride). Even so, the differences of the optimal precipitating condition between A site (Pb and La) and B site (Zr, Sn and Ti) hydroxides tend to result in a stoichiometric problem in the final powders.

In this work, a wet chemical method ceramics using colloidal processing was developed for the preparation of PLZST. Relative low cost start materials were used,

* Corresponding author. Tel.: +86-21-65980230; fax: +86-21-65980230.

E-mail address: chenming@yeah.net (M. Chen).

which makes this method suitable for bulk ceramics preparation. A two-step procedure was designed, in which the precursor site B was prepared by coprecipitation and precursor site A was introduced in the form of an aqueous solution, eliminating the problems in the coprecipitation method as mentioned above.

2. Experimental procedure

2.1. Powders and disc specimens preparation

The composition of $(\text{Pb}_{0.97}\text{La}_{0.02})(\text{Zr}_{0.65}\text{Sn}_{0.25}\text{Ti}_{0.10})\text{O}_3$ at the antiferroelectric to ferroelectric phase boundary in the PLZST ternary system was chosen for the powder preparation, as shown in Fig. 1.

The starting reagents were high purity lead acetate $\text{Pb}(\text{CH}_3\text{COOH})_2 \cdot 3\text{H}_2\text{O}$, lanthanum acetate $\text{La}(\text{CH}_3\text{COOH})_3 \cdot 1\frac{1}{2}\text{H}_2\text{O}$, zirconium oxychloride $\text{ZrOCl}_2 \cdot 8\text{H}_2\text{O}$, stannic chloride $\text{SnCl}_4 \cdot 5\text{H}_2\text{O}$ and titanium tetrachloride TiCl_4 . The flow diagram is given in Fig. 2.

The precursor solution of site B was prepared by first dissolving $\text{ZrOCl}_2 \cdot 8\text{H}_2\text{O}$ and $\text{SnCl}_4 \cdot 5\text{H}_2\text{O}$ in deionized water heated to 80°C , and then allowing TiCl_4 to drip slowly into the hot solution while vigorously stirring. The coprecipitation was achieved by mixing B site precursor solution with an equal volume of aqueous ammonia NH_4OH the concentration of which had been adjusted to maintain the end pH of the mixture at 8.5. The precipitates were then washed with distilled water with the pH adjusted to 8.5 with NH_4OH until no residual Cl^- could be detected by acidified silver nitrate.

The precursor solution of site A, prepared by dissolving $\text{Pb}(\text{CH}_3\text{COOH})_2 \cdot 3\text{H}_2\text{O}$ together with $\text{La}(\text{CH}_3$

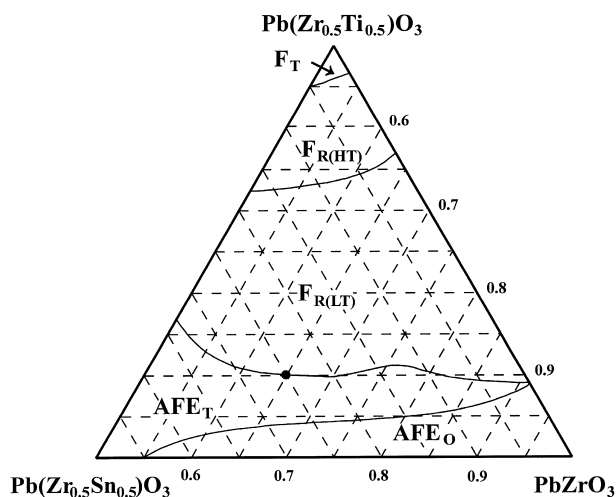


Fig. 1. Ternary phase diagram of $(\text{Pb}_{0.97}\text{La}_{0.02})(\text{Zr}, \text{Sn}, \text{Ti})\text{O}_3$ showing composition in this work. F_T , ferroelectric tetragonal phase; $F_{R(HT)}$, ferroelectric rhombohedral phase (high temperature); $F_{R(LT)}$, ferroelectric rhombohedral phase (low temperature); AFE_T , antiferroelectric tetragonal phase; AFE_O , antiferroelectric tetragonal phase.

$\text{COOH})_3 \cdot 1\frac{1}{2}\text{H}_2\text{O}$ in deionized water, was then mixed with as-washed B site precipitates, adequate acetic acid was added as peptizator to achieve an homogeneous mixture.

The peptizate obtained was, thereafter, heated at 80°C until gelification occurred before being dried at 120°C for 6 h. The dried gel was ground in a mortar and calcined in air from 450 to 650°C for 2 h to determine the optimal calcining condition. Twenty hours planetary ball milling with ZrO_2 media was carried out to reduce the calcined powders to a sub-micron consistency.

The powders obtained were subjected to axial pressing at 200 MPa to form disc specimens of 12 mm in diameter and 0.5 mm in thickness. The disc specimens were sintered from 1000 to 1250°C for 2 h in a lead rich atmosphere. Silver paste was screen printed on the surface of the discs, which were then baked at 700°C to form electrodes.

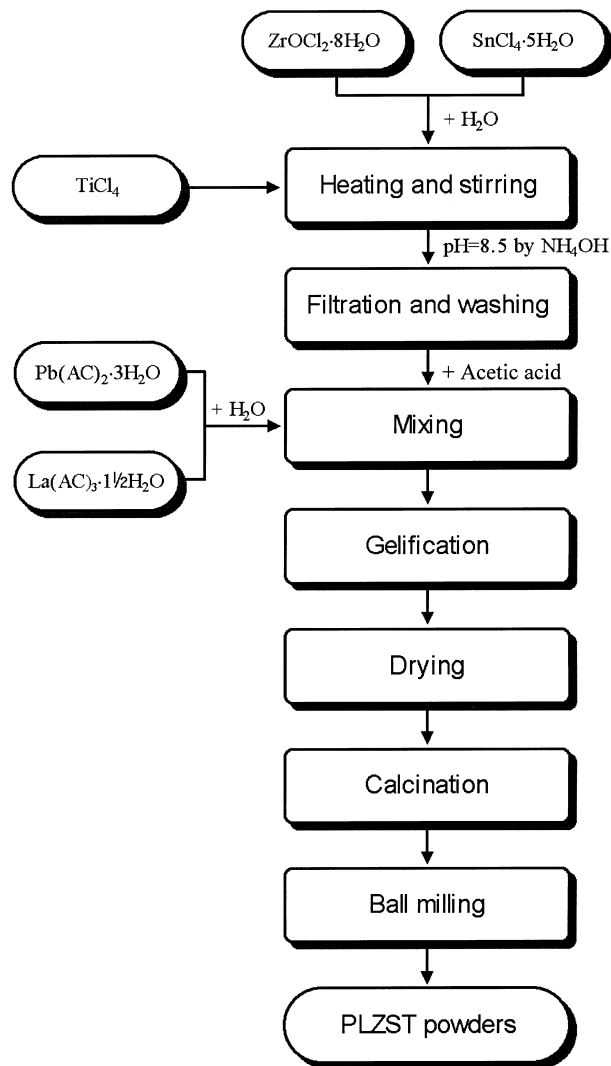


Fig. 2. Flow chart of chemical preparation of $(\text{Pb}, \text{La})(\text{Zr}, \text{Sn}, \text{Ti})\text{O}_3$ ceramic powders.

2.2. Powders and disc specimens characterization

The thermal behavior of as-dried gel was studied by thermogravimetric analysis (TA instruments, TGA 2050) in the temperature range of 30–800°C, using a high resolution dynamic method, and differential scanning calorimetry (TA instruments, DSC 2910) in the temperature range of 30–600°C at a heating rate of diffraction meter (Rigaku, D/max-2400). The stoichiometry of calcined powder was analyzed by X-ray fluorescence technique (Rigaku, 3550 Simultaneous X-Ray Spectrometer System). The distribution of the particle size of powders after 20 h planetary ball milling was measured by a laser particle size analyzer (Cilas, Granulometer 1064).

Relative density of disc specimens after sintering was determined by the water displacement method, and the grain size was measured by scanning electron microscopy (Shimadzu EPMA-8705QH2 electron probe microanalyzer) from fractured surfaces. Hysteresis loop and strain curve were measured using a computer controlled system comprised of a modified Swayer-Tower circuit and a linear variable displacement transformer (LVDT) at room temperature.

3. Results and discussion

Fig. 3 shows the TGA and DSC curves of the as-dried gel. The initial weight loss in the temperature range 25–150°C is attributed to the liberation of occluded water and the gradual decomposition of acetate group, which is accompanied by an endothermic peak in 96.75°C. The minor endothermic peak in 192.67°C is corresponding

to the decomposition temperature of lead acetate. The marked weight loss of the powder from 200 to 400°C may be due to the decomposition of hydroxyl group, which resulted in endothermic peaks observed at 269.68 and 308.57°C. Complete decomposition was observed around 600°C.

Based on the results of TGA and DSC, a series of calcinations were carried out on the dried gel from 450 to 650°C for 2 h. XRD was conducted and the X-ray diffraction patterns of the calcined powder are shown in Fig. 4. The crystalline perovskite phase appears after being calcined at 450°C for 2 h and the complete perovskite phase of PLZST was formed at 600°C for 2 h.

The actual composition of the powder calcined at 550°C for 2 h was analyzed by XRF. The results listed in Table 1 show that PLZST powders prepared by this method have good stoichiometry. After being ball milled, a submicron particle size distribution was achieved as listed in Table 2.

The relative density of disc specimens sintered from 1000 to 1250°C for 2 h was measured and SEM was conducted for the optimization of sintering. As illustrated in Fig. 5, a maximum relative density of 98% was achieved from the specimens sintered at 1100°C for 2 h, and in the temperature range of 1100–1200°C, the relative density exceeds 97%. Fig. 6 shows the SEM photographs of the fractured surfaces from specimens sintered at 1100°C for 2 h. It can be seen that the ceramic body is well densified and average grain size is about 4 µm.

A typical antiferroelectric double hysteresis loop and field-induced strain curve of the specimens sintered at 1100°C for 2 h are illustrated in Fig. 7. The transition

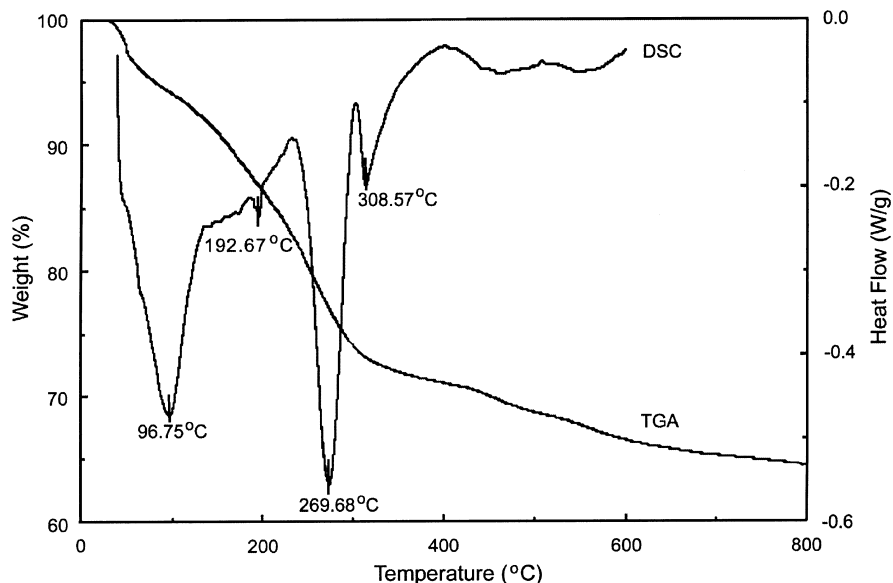


Fig. 3. TGA and DSC curves of $(\text{Pb}_{0.97}\text{La}_{0.02})(\text{Zr}_{0.65}\text{Sn}_{0.25}\text{Ti}_{0.10})\text{O}_3$ dried gel.

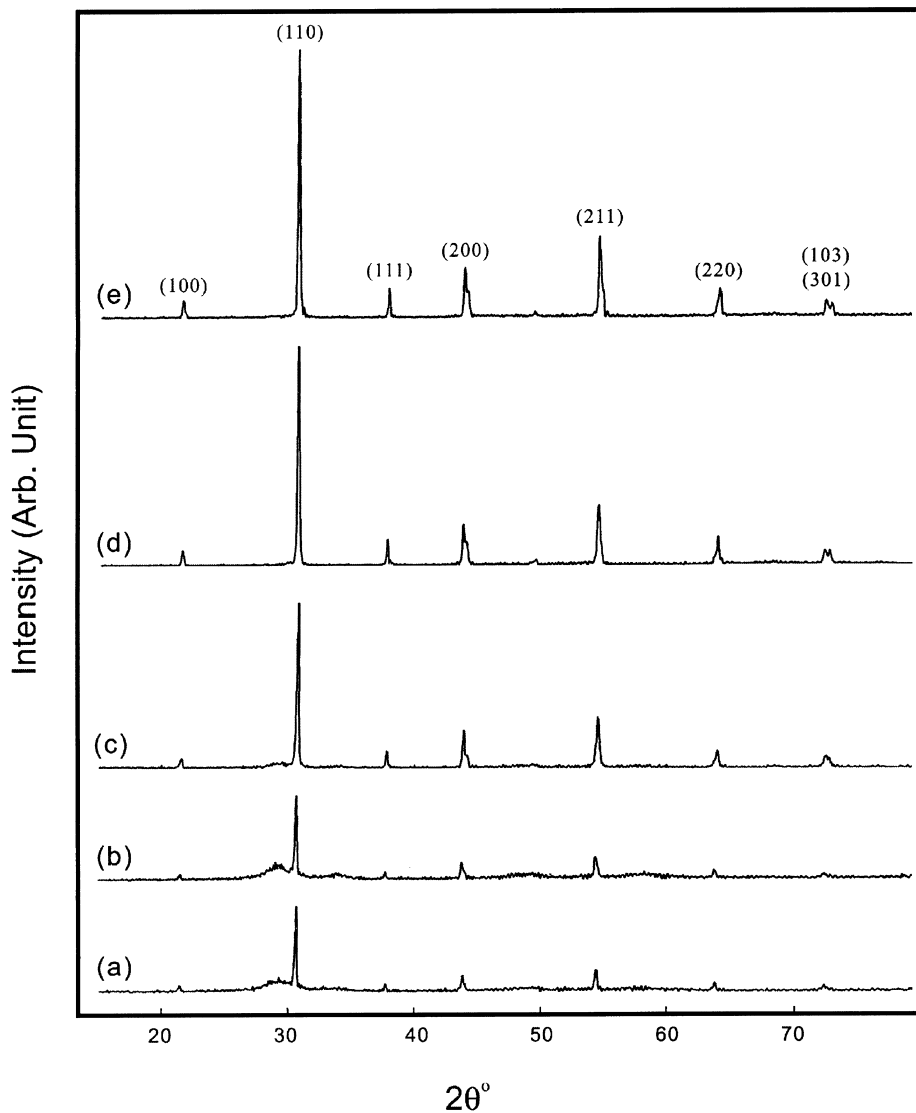


Fig. 4. X-ray diffraction patterns of $(\text{Pb}_{0.97}\text{La}_{0.02})(\text{Zr}_{0.65}\text{Sn}_{0.25}\text{Ti}_{0.10})\text{O}_3$ ceramic powders calcined at (a) 450°C, (b) 500°C, (c) 550°C, (d) 600°C, (e) 650°C for 2 h.

Table 1
XRF analysis of calcined PLZST powder

Element	Composition	Analyzed value
Pb	0.97	0.972
La	0.02	0.018
Zr	0.65	0.643
Sn	0.25	0.262
Ti	0.10	0.092

Table 2
Particle size distribution of PLZST powder after 20 h planetary ball milling

D_{10}	D_{50}	D_{90}	D_{mean}
0.10 μm	0.50 μm	1.01 μm	0.8 μm

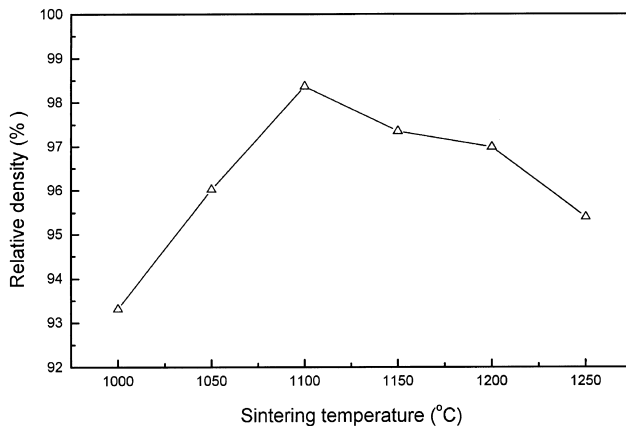


Fig. 5. Relative density of disc specimens sintered at various temperatures for 2 h.

field from antiferroelectric to ferroelectric $E_{\text{AFE-FE}}$ is 4.3 kV/mm and the maximum longitude strain under 6 kV/mm electric field is 0.30%, which are approximately equal to the literature value.¹¹

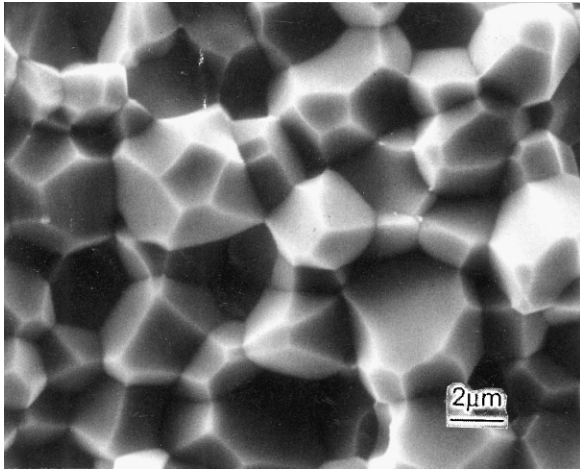


Fig. 6. SEM photograph of fractured surface from the PLZST specimen sintered at 1100°C for 2 h.

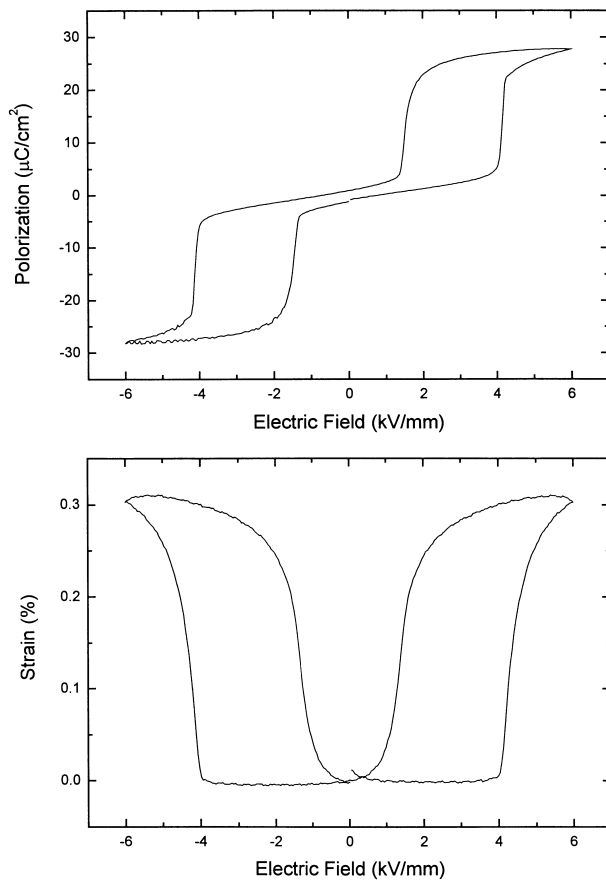


Fig. 7. Antiferroelectric double hysteresis and strain cure of PLZST ceramics with a composition of $(\text{Pb}_{0.97}\text{La}_{0.02})(\text{Zr}_{0.65}\text{Sn}_{0.25}\text{Ti}_{0.10})\text{O}_3$.

4. Conclusions

A two-step wet chemical method using colloidal processing was developed for the preparation of $(\text{Pb}, \text{La})(\text{Zr}, \text{Sn}, \text{Ti})\text{O}_3$ antiferroelectric ceramics. The complete perovskite phase was formed at 600°C for 2 h, and submicron powders were obtained through ball milling. A relative density of 98% was achieved from disc specimens sintered at 1100°C for 2 h, average grain size measured from fracture surfaces is about 4 μm. An antiferroelectric double hysteresis with $E_{\text{AFE-FE}} = 4.3$ kV/mm and a strain curve with maximum longitude strain of 0.30% under a 6 kV/mm electric field were observed from the composition of $(\text{Pb}_{0.97}\text{La}_{0.02})(\text{Zr}_{0.65}\text{Sn}_{0.25}\text{Ti}_{0.10})\text{O}_3$.

Acknowledgements

One of the authors (M.C.) would like to thank Ms. He Ling for XRF and particle size analysis and Ms. Wu Xiaoping for XRD analysis.

References

- Berlincourt, D., Jaffe, H., Krueger, H. H. A. and Jaffe, B., Release of electric energy in $\text{PbNb}(\text{Zr}, \text{Ti}, \text{Sn})\text{O}_3$ by temperature and by pressure-enforced phase transitions. *Appl. Phys. Lett.*, 1963, **3**, 90–98.
- Berlincourt, D., Krueger, H. H. and Jaffe, B., Stability of phase in modified lead zirconate with variation in pressure, electric field, temperature and composition. *Phys. Chem. Solids*, 1964, **25**, 659–674.
- Jaffe, B., Cooke, W. R., Jr. and Jaffe, H., Piezoelectric ceramics. In *Monographs on Non-metallic Solids*. Academic Press, London, 1971, pp. 135–181.
- Cross, L. E., Antiferroelectric–ferroelectric switching in simple ‘Kittle’ antiferroelectrics. *J. Phys. Soc. Jpn.*, 1963, **23**, 77–82.
- Uchino, K. and Nomura, S., Shape memory effect associated with the forced phase transition in antiferroelectrics. *Ferroelectrics*, 1983, **50**, 517–521.
- Pan, W. Y., Zhang, Q., Bhalla, A. and Cross, L. E., Field-forced antiferroelectric-to-ferroelectric switching in modified lead zirconate titanate stannate ceramics. *J. Am. Ceram. Soc.*, 1989, **72**(4), 571–578.
- Akiyama, T. and Fujisawa, E., Field-induced antiferroelectric-to-ferroelectric phase transition of lead niobium zirconate titanate stannate ceramics. *Jpn. J. Appl. Phys.*, 1997, **36** (1), No. 9B.
- Nam, Y.-W. and Yoon, K. H., Phase formation and field-induced strain properties in Y-modified lead zirconate stannate titanate ceramics. *Jpn. J. Appl. Phys.*, 1999, **38**, 5544–5548.
- Yang, P. and Payne, D. A., Thermal stability of field-forced and field-assisted antiferroelectric–ferroelectric phase transformations in $\text{Pb}(\text{Zr}, \text{Sn}, \text{Ti})\text{O}_3$. *J. Appl. Phys.*, 1992, **71**(3), 1361–1367.
- Yang, T., *Field-induced phase transition of $\text{Pb}(\text{Zr}, \text{Sn}, \text{Ti})\text{O}_3$ antiferroelectric ceramics*. PhD thesis, Xi’an Jiaotong University, Xi’an, China (in Chinese).
- Markowski, K., Park, S.-E., Yoshikawa, S. and Cross, L. E., The effect of compositional variations in the lead lanthanum zirconate stannate titanate system on electrical properties. *J. Am. Ceram. Soc.*, 1996, **79**(12), 3297–3304.
- Park, S.-E., Markowski, K., Yoshikawa, S. and Cross, L. E., Effect on electrical properties of barium and strontium additions

- in the lead lanthanum zirconate stannate titanate system. *J. Am. Ceram. Soc.*, 1997, **80**(2), 407–412.
13. Lee, J.-H. and Chiang, Y.-M., Pyrochlore–perovskite phase transformation in highly homogeneous (Pb, La)(Zr, Sn, Ti)O₃ powders. *J. Mater. Chem.*, 1999, **9**, 3107–3111.
 14. Uchino, K., Materials update: advances in ceramic actuator materials. *Materials Letters*, 1995, **22**, 1–4.
 15. Kakegawa, K. and Mohri, J., Preparation of Pb(Zr, Ti)O₃ through the use of cupferron. *J. Am. Ceram. Soc.*, 1984, **67**(1), C2–C3.